ARTICLES

Spatial coupling of nitrogen inputs and losses in the ocean

Curtis Deutsch[1], Jorge L. Sarmiento[2], Daniel M. Sigman[3], Nicolas Gruber[4]† & John P. Dunne[5]

Nitrogen fixation is crucial for maintaining biological productivity in the oceans, because it replaces the biologically available nitrogen that is lost through denitrification. But, owing to its temporal and spatial variability, the global distribution of marine nitrogen fixation is difficult to determine from direct shipboard measurements. This uncertainty limits our understanding of the factors that influence nitrogen fixation, which may include iron, nitrogen-to-phosphorus ratios, and physical conditions such as temperature. Here we determine nitrogen fixation rates in the world's oceans through their impact on nitrate and phosphate concentrations in surface waters, using an ocean circulation model. Our results indicate that nitrogen fixation rates are highest in the Pacific Ocean, where water column denitrification rates are high but the rate of atmospheric iron deposition is low. We conclude that oceanic nitrogen fixation is closely tied to the generation of nitrogen-deficient waters in denitrification zones, supporting the view that nitrogen fixation stabilizes the oceanic inventory of fixed nitrogen over time.

The major algal nutrients NO_3^- and PO_4^{3-} are in short supply throughout the well-lit surface waters of the low-latitude ocean. Although NO_3^- is usually depleted before PO_4^{3-}, the N limitation of productivity may be overcome by organisms capable of converting abundant dissolved N_2 into 'fixed' N available to the wider ecosystem[1]. In oligotrophic regions of the warm subtropical ocean, N_2 fixation has been estimated to account for $\sim$50% of the organic carbon exported from the photic zone[2]. However, a high iron requirement of the enzyme system nitrogenase is believed to prevent N_2-fixing organisms from alleviating widespread N limitation[3]. The iron supply from atmospheric dust deposited at the sea surface has been hypothesized to favour N_2 fixation in the more continentally influenced Atlantic Ocean[4], and during relatively dusty ice ages, potentially increasing the N reservoir and productivity of the ice age ocean and thus lowering CO_2 in the ice age atmosphere (ref. 5).

The environmental controls on N_2 fixation and thus its probable response to past and future climate change would be much clearer if we knew the geographic distribution of this process in the modern ocean. Moreover, the persistent question of whether the sources and sinks of fixed N are in balance[6] awaits a robust estimate for the globally integrated rate of oceanic N_2 fixation. Here we determine both the distribution and global rate of N_2 fixation by taking advantage of one of its signatures in surface waters: a net biological uptake of PO_4^{3-} that occurs in the absence of a stoichiometric uptake of NO_3^-. By interpreting the observed nutrient distributions in the context of an ocean circulation model we find a global rate of N_2 fixation of $\sim$140 $\times$ 10^{12} g of N per year occurring disproportionately in the Pacific Ocean.

Nutrient fluxes and N$_2$ fixation

The biological uptake and remineralization of NO_3^- and PO_4^{3-} in the ocean are traditionally assumed to occur with a nearly constant ratio r_n of 16:1 (ref. 1). This assumption, while valid in the global mean, is clearly violated in the presence of N_2 fixation, which requires PO_4^{3-} uptake but no concomitant uptake of fixed N. In regions where N_2 fixation occurs, the consumption of PO_4^{3-}

unaccompanied by fixed N will cause overall surface nutrient drawdown to have an N:P ratio below r_n, leaving the residual surface nutrient pool increasingly depleted in PO_4^{3-} relative to NO_3^-. A convenient measure of the depletion of PO_4^{3-} relative to the biological NO_3^- requirement is given by $P^\star = PO_4^{3-} - NO_3^-/r_n$, which represents the excess of P relative to the standard N quota (see ref. 7 for a related term, $N^\star$, describing N excess). While nutrient uptake by non-N_2-fixing organisms will on average consume NO_3^- and PO_4^{3-} in a proportion that conserves $P^\star$, N_2 fixation will extract PO_4^{3-} alone, driving a water parcel towards lower $P^\star$.

According to this simple conceptual model, N_2 fixation will be revealed as a reduction in $P^\star$ along the transport path of a surface water mass, and its rate can be estimated by combining the observed distributions of nutrients with information about the rate of ocean circulation and mixing. In the steady state, the excess uptake of PO_4^{3-} is equal to the transport convergence of $P^\star$, written as $-\nabla \cdot \Phi(P^\star)$, where Φ represents nutrient fluxes resulting from all physical transport processes. When the circulation and mixing of the upper ocean results in an excess PO_4^{3-} supply, $-\nabla \cdot \Phi(P^\star) > 0$, a biological uptake of PO_4^{3-} beyond the standard N quota, will be required to bring NO_3^- and PO_4^{3-} back towards their observed concentrations (Fig. 1). To the degree that non-N_2-fixing phytoplankton produce most of the organic matter that actually sinks out of the surface ocean, the rate of N_2 fixation associated with a given excess P supply is well approximated by $J_{fix}(N) \approx -r_n \nabla \cdot \Phi(P^\star)$. However, an exact expression requires two modifications, one that accounts for any direct export of organic matter from N_2-fixing organisms with a high-biomass N:P ratio, and another that incorporates the effect of dissolved organic matter (DOM) cycling on the inferred supply of N and P.

The best-studied and perhaps dominant N_2 fixer in the ocean, *Trichodesmium* spp., has an N:P ratio r_f that is several-fold higher than that of non-N_2-fixing algae (ref. 8). A small fraction of *Trichodesmium* biomass may be directly exported as sinking particles rather than being recycled in surface waters, increasing the amount of newly fixed N that should be attributed to P consumption by

[1]Program on Climate Change, School of Oceanography, University of Washington, Seattle, Washington 98195, USA. [2]Atmospheric and Oceanic Sciences Program, Princeton University, Princeton, New Jersey 08544, USA. [3]Department of Geosciences, Guyot Hall, Princeton University, Princeton, New Jersey 08544, USA. [4]IGPP and Department of Atmospheric and Oceanic Sciences, University of California at Los Angeles, Los Angeles, California 90095, USA. [5]NOAA/Geophysical Fluid Dynamics Laboratory, PO Box 308, Forrestal Campus B Site, Princeton, New Jersey 08542, USA. †Present address: Institute of Biogeochemistry and Pollutant Dynamics, ETH Zurich, Zurich, Switzerland.

Trichodesmium. The relationship between the physical supply of excess PO_4^{3-} and the inferred rate of N_2 fixation can be generalized (see Methods) as $J_{fix}(N) = -\lambda \nabla \cdot \Phi(P^*)$, where λ is a non-dimensional parameter (Supplementary Fig. 1), $\lambda = \dfrac{r_n}{1 - \gamma_e(1 - r_n/r_f)}$, and where γ_e is the fraction of organic matter production that is exported as sinking particles. If all organic matter production is directly exported in sinking particles ($\gamma_e = 1$), any excess physical PO_4^{3-} supply must be consumed and exported by N_2 fixers so that λ is equal to their biomass N:P ratio r_f (Fig. 1a). In contrast, if nutrient recycling is very efficient ($\gamma_e \ll 1$, Fig. 1b), then newly fixed N added to surface waters makes the inferred excess PO_4^{3-} uptake less than the excess physical PO_4^{3-} supply, and λ approaches r_n, as anticipated above. Because of the high degree of nutrient recycling in the low- and mid-latitude ocean, λ is only slightly (0–20%) greater than r_n (Supplementary Fig. 2), and the estimate of N_2 fixation from surface nutrients is only weakly sensitive to r_f. However, N_2 fixation by diazotrophs with both a high-biomass N:P and an unusually high export efficiency, should they be found, would be underestimated by our approach. Given that the standard N:P ratio of 16:1 (the Redfield ratio) actually derives from measurements of total marine particulates[2] and dissolved nutrients[9], an N:P uptake ratio for non-N_2-fixing organisms must be somewhat lower than this to offset the high r_f from the small fraction of N_2-fixing biomass. We find that an r_n of 15:1 yields a global bulk biomass with a Redfield ratio of 16:1.

The disappearance rate of excess P must also be modified to account for the production and subsequent degradation of dissolved organic N (DON) and P (DOP) whose substantial surface reservoirs constitute a second, slower pathway of nutrient recycling over
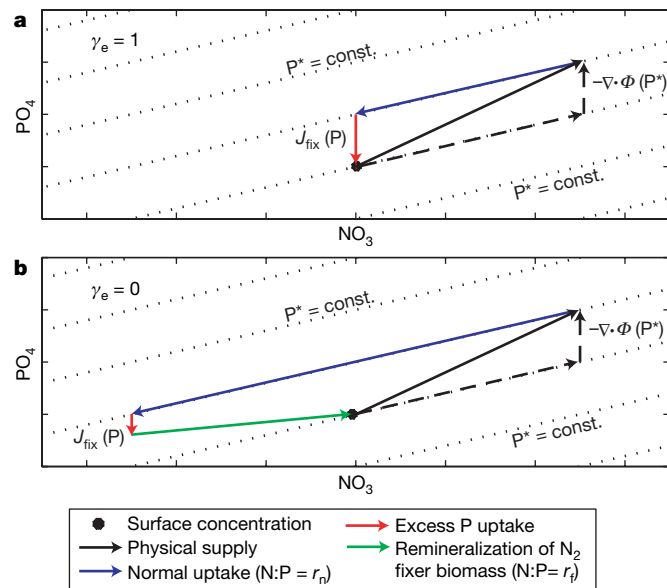
months to years. The impact of DON and DOP on inferred N_2 fixation rates is accommodated (see Methods) by considering the conservation of total fixed N ($N_t = NO_3^- + DON$; excluding NH_4^+ and NO_2^-, which are scarce) and total P ($P_t = PO_4^{3-} + DOP$), whereby P^* is simply replaced by total P^* (P_t^*), the sum of P^* and an analogous DOP^* ($P_t^* = P^* + DOP^* = P_t - N_t/r_n$). Thus, attributing excess PO_4^{3-} uptake to N_2-fixing organisms implies that:

$$J_{fix}(N) = -\lambda \nabla \cdot \Phi(P_t^*)$$

wherever the supply of total P exceeds that of total N times r_n (that is, where $-\nabla \cdot \Phi(P_t^*) > 0$).

The distributions of NO_3^- and PO_4^{3-}, and thus of P^*, are relatively well known[10]. Except in the high-latitude ocean regions, in particular, the Southern Ocean, similar P^* patterns are observed in multiple data sets and therefore represent robust observations (Supplementary Fig. 3). In contrast, the spatial coverage of DON and DOP measurements is insufficient to estimate the transport divergence of DOP^* from those data alone. Instead, we simulate cycles of DON and DOP production and decay in an Ocean General Circulation Model (OGCM) that are driven by observed distributions of NO_3^- and PO_4^{3-} and independently tuned to match the patterns of DON and DOP where they have been most thoroughly studied (see Methods and Supplementary Table 1). The most critical observed pattern is of a tropical excess of DOP ($DOP^* > 0$) and its decline towards a subtropical excess of DON ($DOP^* < 0$) (ref. 11; Supplementary Fig. 4). This requires that, in the model, the fraction of PO_4^{3-} uptake converted to DOP is greater than the fractional production of DON, and that DOP is degraded more rapidly than DON[12].

Global distribution of N_2 fixation

Having accounted for the surface ocean cycling of inorganic and organic nutrients, N_2 fixation can be diagnosed from their physical fluxes computed by assimilating surface NO_3^- and PO_4^{3-} data in the OGCM (see Methods for more details). The climatological distribution of P^* (Fig. 2a) includes high excess PO_4^{3-} concentrations in the Eastern Tropical Pacific, the Subarctic North Pacific, the Arabian Sea, and off the western coast of Africa. In all of these regions, NO_3^- is consumed through denitrification (defined here as the sum of all processes that convert fixed N to N_2) in subsurface waters, rendering them enriched in PO_4^{3-} relative to NO_3^-. Excess PO_4^{3-} declines towards zero in the subtropical gyre of the North Pacific, throughout the North Atlantic and, to a lesser degree, in the southern subtropical gyres of all three ocean basins. This P^* distribution, in the context of the OGCM circulation that transports high-P^* waters into the lower-P^* subtropical gyres, leads to diagnosed rates of N_2 fixation that are focused in the low-latitude ocean (Fig. 2b, c). In the subtropical gyres, our results indicate that ~50% of the particulate N that is exported from the surface layer is newly fixed (as opposed to originating from nitrate supplied by the circulation, see Fig. 2d)[3], making N_2 fixation the dominant N supply that sustains biological carbon export in these systems. The latitudinal pattern of N_2 fixation conforms broadly to the observed biogeography of *Trichodesmium* spp.[13], which thrives in warm, low-nutrient waters. One inference from this result is that either *Trichodesmium* contributes most to global marine N inputs, or that environmental controls on the abundance of *Trichodesmium* are also operating on other N_2-fixing organisms[14].

The cycling of DOM has little net effect on integrated N_2 fixation rates (Table 1) mostly influencing its regional distribution within each basin (Fig. 2c compared to Fig. 2b). The relatively rapid production and degradation of DOP reduces the inferred excess of gross PO_4^{3-} uptake in productive regions while enhancing it in the 'downstream' oligotrophic regions, effectively shifting inferred N_2 fixation away from the tropical upwelling zones and into the subtropical gyres (Fig. 2c) compared to estimates that either neglect DOM (Fig. 2b) or
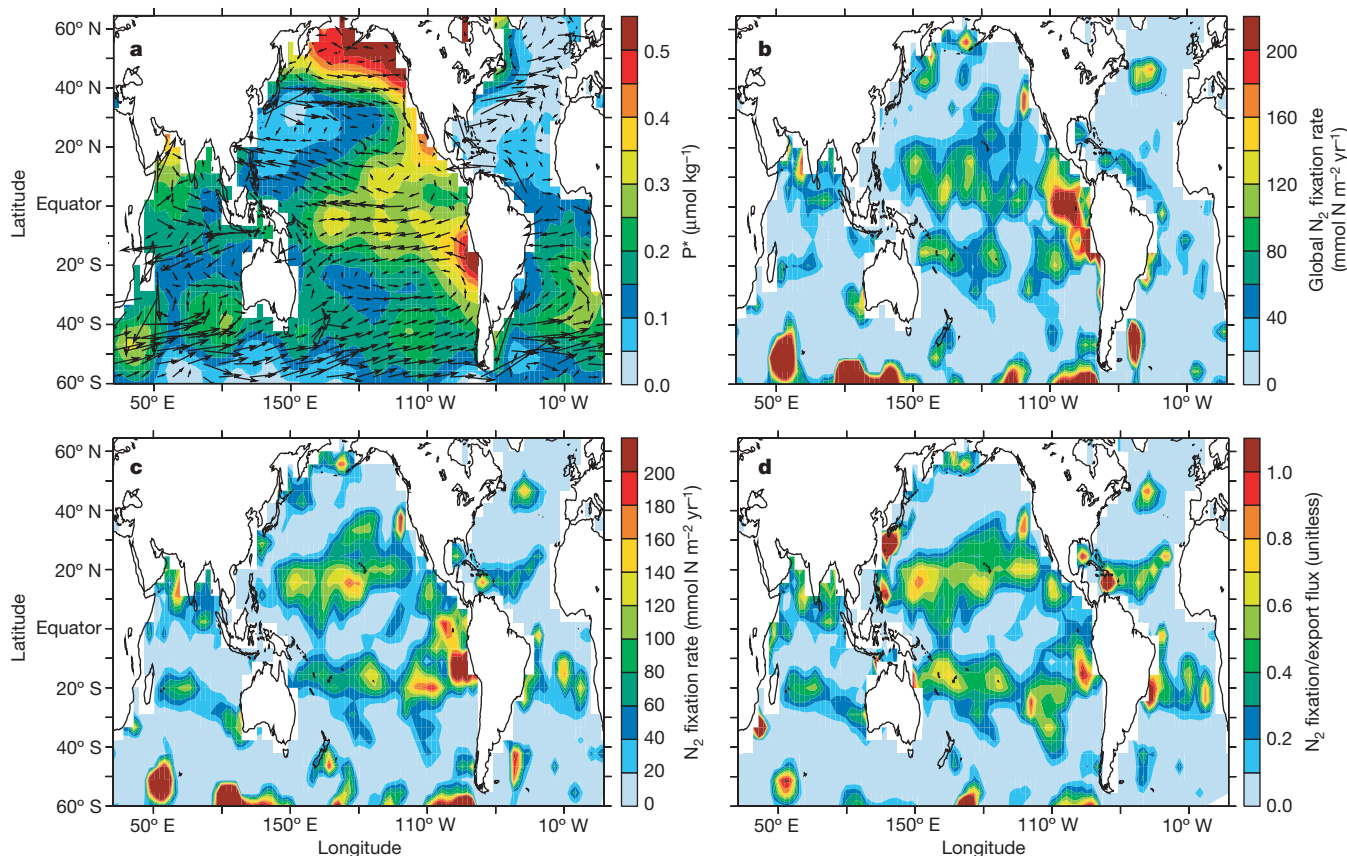

Figure 1 | Schematic depiction of method to determine N_2 fixation from NO_3^- and PO_4^{3-} uptake. Nutrient supply due to ocean circulation (black arrow) with an N:P ratio below r_n (dotted lines), indicates an excess supply of PO_4^{3-} ($-\nabla \cdot \Phi(P^*) > 0$, vertical dashed arrow) compared to normal biological N:P requirements (dashed arrow with constant P^*). The total nutrient uptake required to balance the physical nutrient supply can be interpreted as a non-N_2-fixing component that occurs with an N:P ratio of r_n (blue arrow), plus an excess of PO_4^{3-} uptake (red arrow) due to N_2-fixing organisms. When all nutrient uptake is rapidly exported (**a**), each mole of excess P uptake by N_2 fixers carries r_f moles of newly fixed N to depth without altering the surface N supply. However, when nutrients are recycled in surface waters (**b**), the newly fixed N added to surface waters (green arrow) supplements the physical N supply, effectively reducing the excess PO_4^{3-} supply. The effect of nutrient recycling on N_2 fixation rates inferred from a given nutrient supply depends on r_f, assumed here to be 50:1, and the fraction of total nutrient uptake exported in sinking particles (γ_e), assumed to be 1 in **a** and 0 in **b**. The combined effect of these parameters is represented by λ.

Figure 2 | Annual mean distribution of P*, ocean currents, and the N$_2$ fixation rates determined from them at 0–120 m depth. a, The P* distribution (P* = PO$_4^{3-}$ − NO$_3^-/r_n$) is based on climatological data from the World Ocean Atlas[10], and the surface velocity is computed from the MOM3 ocean general circulation model[30]. **b,** Global N$_2$ fixation rates diagnosed from the convergence of excess inorganic PO$_4^{3-}$, $-\lambda\nabla\cdot\Phi(P^*)$,

which requires an excess uptake of PO$_4^{3-}$ relative to the biological N requirement. **c,** Rates of N$_2$ fixation accounting for both inorganic and organic nutrient pools, equal to $-\lambda\nabla\cdot\Phi(P_t^*)$ where this term is positive (that is, where excess P$_t$ converges). **d,** N$_2$ fixation rates (from **c**) as a fraction of the export flux of organic matter.

assume proportional production and decay of DON and DOP (Supplementary Fig. 5). On the basis of the complete calculation including the DOM cycle (Fig. 2c), N$_2$ fixation appears to be proximal to but does not overlap with regions of non-zero nutrients. However, given data coverage and the likelihood of unresolved seasonality, we avoid using its detailed distribution to address whether N$_2$ fixation can occur in nutrient-replete waters.

The occurrence of maximum inferred N$_2$ fixation rates in tropical and subtropical latitudes is highly consistent with previous views[13], but its inter-basin distribution is not. Whereas there is a widely held

Table 1 | Global and basin-scale N$_2$ fixation rates diagnosed from surface nutrients

Model description	N$_2$ fixation rate (10^{12} g N yr^{-1})		
	Pacific (130×10^{12} m^2)	Atlantic (63×10^{12} m^2)	Global (240×10^{12} m^2)
Standard Model	95	20	137
No DOM	95	15	130
Alternative P* (WOCE)	93	21	143
Alternative circulation (winds)	108	17	151
Alternative circulation (mixing)	98	13	140
Assume $r_n = 16$	107	25	158

Rates are integrated over the top 120 m from 40° S to 65° N for several models: the Standard Model, a model without DOM, and four sensitivity experiments (see Supplementary Information), in which the effect of uncertainty in physical nutrient transport is estimated using an alternative P* distribution (based on quality-controlled nutrient data from the World Ocean Circulation Experiment, WOCE) and two alternative circulations (one that is forced by an alternate pattern of wind stress, and one that additionally imposes higher rates of mixing). These calculations, together with one in which the N:P uptake ratio for non-N$_2$-fixing plankton (r_n) is assumed to be 16:1, reveal a pattern and global rate of N$_2$ fixation that is robust with respect to the key methodological uncertainties.

expectation of higher rates in the Atlantic[4], our estimates imply areal rates of N$_2$ fixation in the Pacific Ocean more than twice as high as those in the Atlantic, with intermediate values in the Indian Ocean (Table 1). The Pacific hosts over two-thirds of the total ∼140 Tg (1 Tg = 10^{12} g) of new N required each year to account for the excess uptake of PO$_4^{3-}$, followed by 16% of the total in the Indian Ocean. Denitrification in the eastern tropical Pacific[15], subarctic North Pacific[16] and Arabian Sea[17] generates nutrient-rich and NO$_3^-$-deficient waters that subsequently undergo a disproportionate loss of PO$_4^{3-}$ as they are upwelled and transported into the adjacent subtropical gyres. In contrast, the relatively weak P* gradients found across much of the subtropical North Atlantic require nutrient uptake with N:P ratios that are close to or even greater than r_n. Our basin-wide N$_2$ fixation rate for the Pacific (48 mmol N m^{-2} yr^{-1}, averaged from 40° S to 65° N) is similar to previous estimates (∼50 mmol N m^{-2} yr^{-1}; refs 1, 18). In the Atlantic, our estimate of 23 mmol N m^{-2} yr^{-1} is at the low end of the range of previous studies based on thermocline nutrient stoichiometry (30 to 72 mmol N m^{-2} yr^{-1}; refs 7, 19), and is also less than a recent estimate (87 mmol N m^{-2} yr^{-1}) from *in situ* measurements in the western tropical North Atlantic[20], although these studies examined a more selective area, where average rates can be expected to be higher.

We have investigated the sensitivity of our results to uncertainties in ocean circulation, the distribution of P*, and the N:P ratio of non-N$_2$ fixing plankton, r_n. We find that globally integrated N$_2$ fixation rates among the sensitivity experiments vary by less than 25% (Table 1). While the details of the inferred distribution of N$_2$ fixation may vary, the partitioning between ocean basins is robust, with the Atlantic consistently contributing 15% or less to the global input

(Supplementary Figs 7, 8). The greatest dependence of the global N_2 fixation rate is on r_n. For a given ratio of total nutrient drawdown, a higher N:P ratio among non-N_2-fixing organisms requires a greater fraction of P uptake to be attributed to diazotrophs (Table 1); however, the large-scale distribution of inferred N_2 fixation is not changed.

Internal regulation of oceanic fixed N

The pattern of N_2 fixation diagnosed from surface nutrients (Fig. 2c) has several important implications for the understanding of environmental controls on marine N_2 fixation. The inter-basin differences in diagnosed N_2 fixation rates are opposite to those for iron supplied through atmospheric dust deposition[21], which is higher in the Atlantic than in the Pacific. This suggests that the supply of iron may not be a primary limiting factor for marine N_2 fixation, or that the supply of iron from the subsurface compensates for low atmospheric inputs in the Pacific. Instead, regions of N_2 fixation diagnosed from surface nutrient transport are closely connected to zones of low O_2 and active denitrification in the water column[17,22]. This suggests that NO_3^- deficits generated in the suboxic zones of the Pacific and Indian Oceans and subsequently transported to surface waters provide an important stimulus for N_2 fixation, perhaps by increasing the ability of N_2 fixers to compete with other phytoplankton.

The relatively tight coupling between denitrification and N_2 fixation inferred from this analysis in turn offers support for a previously hypothesized negative feedback in the N budget, whereby any externally driven increase or decrease in the oceanic N reservoir will be counteracted by a decrease or increase in the rate of N_2 fixation, respectively[1,23]. For example, our results support the hypothesis that N_2 fixation responded to the reconstructed surge in water column denitrification at the end of the last ice age by increasing in step[24]. Moreover, given the close geographic proximity of denitrification and N_2 fixation noted here, this response could have occurred on a timescale of years to decades, which is nearly instantaneous on the timescale of glacial–interglacial transitions. Finally, this compensation would occur within individual ocean basins, not requiring that, for instance, changes in Pacific denitrification were countered by comparably large changes in Atlantic N_2 fixation.

The proximity of denitrification and N_2 fixation centres suggests that the stabilizing N-to-P feedback would have been operating over recent decades while the ocean N budget has been studied. If so, this argues against the interpretation that the recognized difference between the estimated inputs and outputs of oceanic fixed N could be explained as high-frequency transient imbalances within a longer-term steady state[25]. Rather, our results argue against any such imbalance. At the same time, our globally integrated estimate for oceanic N_2 fixation, like previous estimates, is far below many current estimates for total denitrification (for example, $\sim$350 Tg of N per year[26]). Taking our results at face value, either the estimates for fixed N loss must be too large, or we must be missing a major additional input of N to the ocean.

METHODS

Nutrient mass balance. The rate of N_2 fixation diagnosed from surface nutrients can be generalized by considering the conservation of inorganic nutrients and DOM in surface waters:

$$\frac{\partial P}{\partial t} + \nabla \cdot \Phi(P) = J_{DOM}(P) - J_{up}(P) + J_{regen}(P) \tag{1}$$

$$\frac{\partial N}{\partial t} + \nabla \cdot \Phi(N) = J_{DOM}(N) - J_{up}(N) + J_{regen}(N) \tag{2}$$

$$\frac{\partial DOP}{\partial t} + \nabla \cdot \Phi(DOP) = -J_{DOM}(P) + \gamma_P J_{up}(P) \tag{3}$$

$$\frac{\partial DON}{\partial t} + \nabla \cdot \Phi(DON) = -J_{DOM}(N) + \gamma_N[J_{fix}(N) + J_{up}(N)] \tag{4}$$

where P and N are the respective concentrations of inorganic PO_4^{3-} and inorganic fixed N, which is dominated by NO_3^- ($N = NH_4^+ + NO_2^- +$

$NO_3^- \approx NO_3^-$). The $\nabla \cdot \Phi$ terms represent the divergence of physical fluxes due to advection and diffusion, and the J terms represent biological sources and sinks of nutrients. J_{up} is total nutrient uptake including that associated with N_2 fixation, J_{DOM} is the degradation of DON and DOP, J_{regen} is the instantaneous regeneration of surface nutrients, and $J_{fix}(N)$ is the fixation of N_2 into organic N. A fraction γ_N of total primary N production, $J_{fix}(N) + J_{up}(N)$, is converted to DON, while a distinct fraction of gross P uptake γ_P is converted to DOP. The fraction of organic matter production that sinks as particulate organic matter is denoted γ_e, so that the regenerated nutrient flux is what remains:

$$J_{regen}(P) = (1 - \gamma_e - \gamma_P)J_{up}(P) \tag{5}$$

$$J_{regen}(N) = (1 - \gamma_e - \gamma_N)(J_{up}(N) + J_{fix}(N)) \tag{6}$$

In contrast to P, surface N regeneration and DON production may introduce exogenous, newly fixed N from N_2 fixation. Equations (1)–(5) can be combined to describe the conservation of total phosphorus ($P_t = P + DOP$), and total fixed nitrogen ($N_t = N + DON$):

$$\frac{\partial P_t}{\partial t} + \nabla \cdot \Phi(P_t) = -\gamma_e J_{up}(P) \tag{7}$$

$$\frac{\partial N_t}{\partial t} + \nabla \cdot \Phi(N_t) = -\gamma_e J_{up}(N) + (1 - \gamma_e)J_{fix}(N) \tag{8}$$

Equations (7) and (8) state that the time rate-of-change and transport divergence of P_t is balanced by the sinking flux (export) of P, and similarly for N_t, except that there is also a source of N_t from the fraction of newly fixed N that does not get exported.

Our fundamental assumption is that N_2 fixation can be estimated from (see Fig. 1):

$$J_{fix}(N) = r_f(J_{up}(P) - \frac{J_{up}(N)}{r_n}) \tag{9}$$

where r_n is the N:P ratio of 'normal' nutrient uptake and r_f is the N:P ratio of N_2 fixers. Therefore, N_2 fixation can be diagnosed (in the steady state) using equations (7)–(9) from:

$$J_{fix}(N) = -\lambda \nabla \cdot \Phi(P_t^*) \text{ only if } -\nabla \cdot \Phi(P_t^*) > 0 \tag{10}$$

where $-\nabla \cdot \Phi(P_t^*)$ is the convergence of P_t^* due to circulation, and $\lambda = r_n[1 - \gamma_e(1 - r_n/r_f)]^{-1}$ can be thought of as the amount of N that must be fixed to compensate a given excess physical supply of PO_4^{3-}. Its dependence on r_f has two opposing effects. On the one hand, the amount of N fixed per unit of PO_4^{3-} uptake by N_2 fixers increases with r_f, so that, for a higher r_f a given burden of excess PO_4^{3-} supplied by the circulation is associated with a higher N_2 fixation rate. On the other hand, as r_f increases, the net excess of PO_4^{3-} supplied to the surface ocean decreases owing to higher *in situ* N inputs from N_2 fixers. Thus, the amount of N_2 fixation required to balance a given supply of excess PO_4^{3-} inferred from nutrient distributions and ocean flow fields depends on both the N:P ratio of N_2-fixing biomass (an increase in the N:P ratio will increase the amount of N_2 fixed) and the degree of nutrient recycling (an increase in which will reduce the amount of N_2 fixed, and more so for a higher r_f). Because the expression inside the square brackets is close to 1, the value of λ tends to be close to that of r_n (Supplementary Fig. 2).

Ocean circulation/biogeochemistry model. We compute physical and biological nutrient fluxes within an ocean biogeochemical/general circulation model that integrates the conservation equations (1)–(4) to a steady state. Model NO_3^- and PO_4^{3-} concentrations are damped towards climatological values (Fig. 2a), providing an estimate of gross nutrient uptake rates. An excess uptake of P is attributed to N_2-fixing organisms with an N:P ratio of 50:1; see equation (9). We assume that regions with an excess of N supply relative to P (that is, $-\nabla \cdot \Phi(P^*) < 0$; Supplementary Fig. 8) are balanced by high N:P uptake[27]. An alternative explanation would be that biological nutrient uptake occurs at the standard ratio but that an additional process, such as denitrification, removes N but not P. This could occur in regions where denitrifying sediments are found in the shallow water column, for example, in the subarctic North Pacific[28].

The fraction of total productivity that is exported in sinking particles (γ_e) is determined through an empirical model in which γ_e is an increasing function of productivity and a decreasing function of surface temperature (Supplementary Fig. 2)[29]. DON and DOP are produced in proportion to N and P uptake via the parameters γ_N and γ_P, and consumed in a first-order decay process (that is, $J_{DOM}(N) = DON/\tau_{DON}$ and $J_{DOM}(P) = DOP/\tau_{DOP}$; see the 'Nutrient mass balance' section of the Methods) that is tuned to match the available observations (see Supplementary Table 1). Tropical/subtropical DON and DOP maxima are most accurately reproduced when the fractional production of DON and DOP (γ_N and γ_P) are 6% and 25%, respectively, and their degradation timescales

(τ_{DON} and τ_{DOP}) are 2 and 0.5 years, respectively. By tuning the parameters for DOM cycling and restoring N and P distributions towards observations, we ensure that the transport of N, P, DON and DOP is maximally consistent with observed values. Tracer transport is computed within a coarse-resolution ($\sim 4°$) general circulation model, the Modular Ocean Model (MOM3). We adopt here the model configuration P2A, in which both the upper-ocean thermal structure and global new production rates are consistent with observational constraints[30].

1. Redfield, A. C., Ketchum, B. H. & Richards, F. A. in *The Sea* (ed. Hill, M. N.) Vol. 2, 26–77 (Interscience, New York, 1963).
2. Karl, D. *et al.* The role of nitrogen fixation in biogeochemical cycling in the subtropical North Pacific Ocean. *Nature* **388**, 533–538 (1997).
3. Falkowski, P. G. Evolution of the nitrogen cycle and its influence on the biological sequestration of CO_2 in the ocean. *Nature* **387**, 272–275 (1997).
4. Karl, D. *et al.* Dinitrogen fixation in the world's oceans. *Biogeochemistry* **57/58**, 47–98 (2002).
5. Broecker, W. S. & Henderson, G. M. The sequence of events surrounding Termination II and their implications for the cause of glacial-interglacial CO_2 changes. *Paleoceanography* **13**, 352–364 (1998).
6. Codispoti, L. A. Biogeochemical cycles—Is the ocean losing nitrate? *Nature* **376**, 724 (1995).
7. Gruber, N. & Sarmiento, J. L. Global patterns of marine nitrogen fixation and denitrification. *Glob. Biogeochem. Cycles* **11**, 235–266 (1997).
8. Letelier, R. M. & Karl, D. M. *Trichodesmium* spp. physiology and nutrient fluxes in the North Pacific subtropical gyre. *Aquat. Microb. Ecol.* **15**, 265–276 (1998).
9. Anderson, L. A. & Sarmiento, J. L. Redfield ratios of remineralization determined by nutrient data analysis. *Glob. Biogeochem. Cycles* **8**, 65–80 (1994).
10. Conkright, M. E. *et al. World Ocean Atlas 2001: Objective Analyses, Data Statistics, and Figures, CD-ROM Documentation* 1–17 (National Oceanographic Data Center, Silver Spring, 2002).
11. Abell, J., Emerson, S. & Renaud, P. Distributions of TOP, TON and TOC in the North Pacific subtropical gyre: Implications for nutrient supply in the surface ocean and remineralization in the upper thermocline. *J. Mar. Res.* **58**, 203–222 (2000).
12. Wu, J. F., Sunda, W., Boyle, E. A. & Karl, D. M. Phosphate depletion in the western North Atlantic Ocean. *Science* **289**, 759–762 (2000).
13. Capone, D. G., Zehr, J. P., Paerl, H. W., Bergman, B. & Carpenter, E. J. *Trichodesmium*, a globally significant marine cyanobacterium. *Science* **276**, 1221–1229 (1997).
14. Zehr, J. P. *et al.* Unicellular cyanobacteria fix N_2 in the subtropical North Pacific Ocean. *Nature* **412**, 635–638 (2001).
15. Codispoti, L. A. & Richards, F. A. An analysis of the horizontal regime of denitrification in the eastern tropical North Pacific. *Limnol. Oceanogr.* **21**, 379–388 (1976).
16. Lehmann, M. F. *et al.* Origin of the deep Bering Sea nitrate deficit: Constraints from the nitrogen and oxygen isotopic composition of water column nitrate and benthic nitrate fluxes. *Glob. Biogeochem. Cycles* **19**, doi:10.1029/2005GB002508 (2005).
17. Brandes, J. A., Devol, A. H., Yoshinari, T., Jayakumar, D. A. & Naqvi, S. W. A. Isotopic composition of nitrate in the central Arabian Sea and eastern tropical North Pacific: a tracer for mixing and nitrogen cycles. *Limnol. Oceanogr.* **43**, 1680–1689 (1998).
18. Deutsch, C., Gruber, N., Key, R. M., Sarmiento, J. L. & Ganaschaud, A. Denitrification and N_2 fixation in the Pacific Ocean. *Glob. Biogeochem. Cycles* **15**, 483–506 (2001).
19. Hansell, D. A., Bates, N. R. & Olson, D. B. Excess nitrate and nitrogen fixation in the North Atlantic Ocean. *Mar. Chem.* **84**, 243–265 (2004).
20. Capone, D. G. *et al.* Nitrogen fixation by *Trichodesmium* spp.: An important source of new nitrogen to the tropical and subtropical North Atlantic Ocean. *Glob. Biogeochem. Cycles* **19**, doi:10.1029/2004GB002331 (2005).
21. Mahowald, N. *et al.* Dust sources and deposition during the last glacial maximum and current climate: A comparison of model results with paleodata from ice cores and marine sediments. *J. Geophys. Res. Atmos.* **104**, 15895–15916 (1999).
22. Sigman, D. M. *et al.* Coupled nitrogen and oxygen isotope measurements of nitrate along the eastern North Pacific margin. *Glob. Biogeochem. Cycles* **19**, doi:10.1029/2005GB002458 (2005).
23. Gruber, N. in *Carbon-Climate Interactions* (eds Follows, M. & Oguz, T.) 97–148 (John Wiley & Sons, New York, 2003).
24. Deutsch, C., Sigman, D. M., Thunell, R., Meckler, A. N. & Haug, G. H. Isotopic Constraints on the Glacial/Interglacial Oceanic Nitrogen Budget. *Glob. Biogeochem. Cycles* **18**, doi:10.1029/2003GB002189 (2004).
25. Codispoti, L. A. *et al.* The oceanic fixed nitrogen and nitrous oxide budgets: Moving targets as we enter the anthropocene? *Sci. Mar.* **65**, 85–101 (2001).
26. Brandes, J. A. & Devol, A. H. A global marine fixed nitrogen isotopic budget: Implications for Holocene nitrogen cycling. *Glob. Biogeochem. Cycles* **16**, doi:10.1029/2001GB001856 (2002).
27. Sarmiento, J. L. & Gruber, N. *Ocean Biogeochemical Dynamics* 118–119 (Princeton Univ. Press, Princeton, 2006).
28. Tanaka, T. N deficiency in a well-oxygenated cold bottom water over the Bering Sea shelf: Influence of sedimentary denitrification. *Contin. Shelf Res.* **24**, 1271–1283 (2004).
29. Dunne, J. P., Armstrong, R. A., Gnanadesikan, A. & Sarmiento, J. L. Empirical and mechanistic models for the particle export ratio. *Glob. Biogeochem. Cycles* **19**, doi:10.1029/2004GB002390 (2004).
30. Gnanadesikan, A., Slater, R. D., Gruber, N. & Sarmiento, J. L. Oceanic vertical exchange and new production: a comparison between models and observations. *Deep-Sea Res. II* **49**, 363–401 (2002).